National Technical University of Athens

Department of applied mathematics and physical sciences

Technology of Detectors and Accelerators

Time Projection Chambers (TPCs)

Author:
Georgia Zachou

Student ID:
ge19098

Contents

Abstract

In this assignment we will comprehensively analyze the technological systems behind the detection of the elementary particles and more specifically, we will go through the TPC detector or else Time Projection Detector.

1 Introduction

In the context of subatomic particles exploration, hundreds of techniques and tools have been developed. Instruments known as particle detectors play an outstanding role in capturing and analyzing the characteristics of those particles. In this assignment, we will be analyzing specifically the Time Projection Chamber (TPC), which stands out as a remarkable tool for its unique capabilities in reconstructing particle trajectories and interactions in three dimensions. The TPC is a detector that is based on gas and liquid ionization processes to create reconstructions of the particles trajectories on the 3D space. The whole process includes electromagnetic fields that interact with charged particles and mark their paths inside the chamber.
Before we go through the engineering analysis and the details of such detectors, it is important to mention a few things about its origins. The TPC was invented by David R. Nygren, an American particle physicist, at Lawrence Berkeley Laboratory in the late 1970s. He and his partner Gideon Rahmiel, originally conceived the idea of having a gaseous medium, such as a noble gas, as a detector material. They proposed the concept of electron drift in a gas as a means to record the paths of charged particles, since they would ionize the atoms of the gas, and thus electrons can be drifted towards a readout system. This idea was brilliant. So they started the first TPC development at Lawrence Berkeley National Laboratory in the early 1970s, and by the mid-1970s they had already ran it and tested it.
What G. Rahmiel and D.R. Nygren invented was a crucial step for the future of particle physics back then. Such detection technologies were soon developed in institutes all over the world, and this resulted in the designs being enhanced not only in modeling but also in performance. One of the most famous detectors of that type is the well-known ALICE TPC at CERN.

2 Basic Principles of TPC

2.1 Energy loss of charged particles

Before checking out the structure and the operation of a TPC, it is essential to lay down the foundational physical and mathematical principles that surround its functionality.
To begin with, when charged particles traverse a medium, they face energy losses due to phenomena that are formed, such as atomic excitation, ionization and even bremsstrahlung radiation at low energies. The equation that has been proven to best describe such losses is the well-known Bethe-Bloch equation:

$$\frac{dE}{dx} = Kz^2 \frac{Z}{A} \frac{1}{\beta^2} \left[\frac{1}{2} \ln \left(\frac{2m_e c^2 \beta^2 \gamma^2 T_{\max}}{I^2} \right) - \beta^2 - \frac{\delta(\beta\gamma)}{2} \right] \tag{2.1.1}$$

where :

- $\frac{dE}{dx}$: Rate of energy loss per unit path length,
- $K = 4\pi N_A r_e 2 m_e c^2$, r_e is electron classical radius: Constant (approximately $0.307\,\mathrm{MeV\ g^{-1}\,cm^2}$),
- z: Charge of the incident particle,
- Z: Atomic number of the material,
- A: Atomic mass of the material,
- β: Velocity of the incident particle relative to the speed of light,
- γ: Lorentz factor,
- δ: A correction factor, that is function of both β and γ.

- m_e: Electron rest mass,
- c: Speed of light,
- $T_{\max}$: Maximum kinetic energy transferred to an electron in a single collision, and
- I: Mean excitation energy of the material.

The Bethe-Bloch equation describes the totality of losses and even takes into consideration the δ-electrons as long as they have energy below T_{max}. For someone that is interested in studying the ionization close to the particle's trajectory, they can replace T_{max} with a cut-off value, T_{cut}, that is smaller than the first, and apply it normally in the initial Bethe-Bloch equation. However, we have to mention w, the mean energy loss to produce an electron/ion pair: $w = \frac{\left\langle \frac{dE}{dx} \right\rangle}{n_T}$ (n_T: total number of ion/electron pairs), before we introduce the ionization procedure.
For the rare gases, one can find that $w = (1.4 - 1.8)E_I$ and for the common molecular gases it's $w = (2.1 - 2.5)E_I$ the difference in the E_I comes from the excitation losses and due to slow electron (δ-electrons).

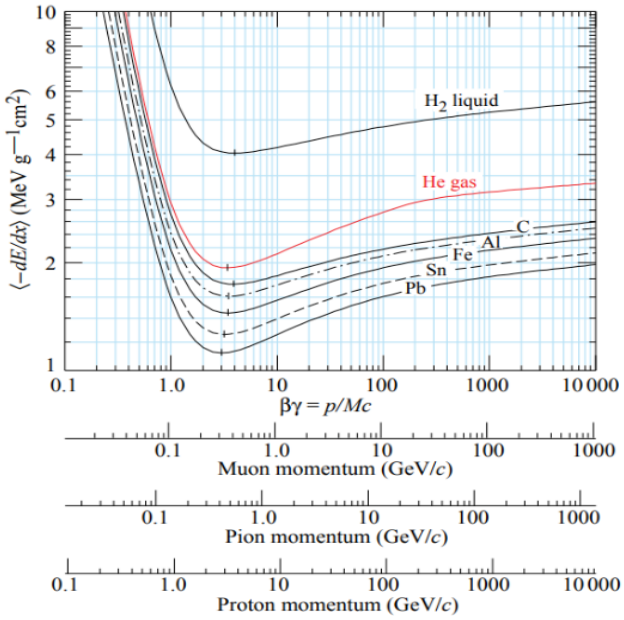

Figure 1: Example for mean energy loss rate in liquid H_2, gaseous He, Carbon aluminium etc.

From the figure 1 one can determine the particle speed β from the sudden decrease of the curve, its momentum p from the increasing curved tracking and even their masses. In this way, one can identify the particle type using those information.

2.2 Ionization of gas

Ionization is the core mechanism of a gas detector, such as TPC. The equation that describes the procedure is:

$$X + p \rightarrow X^+ + p + e^- \tag{2.2.1}$$

Where X are the **gas atoms**, p are the **traversing protons** and e^- are the **δ-electrons**. The procedure (2.1.1) corresponds to the so-called **primary ionization** process.
In case the energy of the δ-electrons is higher than the corresponding ionization energy ($E_\delta > E_i$), we observe a **secondary ionization** between the δ-electrons and the gas atoms:

$$X + e^- \rightarrow X^+ + e^- + e^- \tag{2.2.2}$$

Now the total amount of particles ionized is given from the equation:

$$n_{total} = n_{primary} + n_{secondary} = \frac{\Delta E}{W_i} = \frac{\frac{dE}{dx}\Delta x}{W_i} \tag{2.2.3}$$

where ΔE is the total energy loss, and W_i mean energy loss per produced ion pair (almost equal to 30eV). As $\frac{dE}{dx}$ we define the energy loss per length unit from Bethe-Bloch formula which we explained in the previous subsection.
The table below includes some examples of the characteristics we mentioned above, for some types of gases:

Gas	n_p	n_T	$w\,(eV)$	$E_i\,(eV)$	$E_x\,(eV)$	$\rho\,(mg/cm^3)$
He	4.8	7.8	45	24.5	19.8	0.166
Ne	13	50	30	21.6	16.7	0.84
Ar	25	100	26	15.7	11.6	1.66
Xe	41	312	22	12.1	8.4	5.50
CH_4	37	54	30	12.6	8.8	0.67
C_2H_6	48	112	26	11.5	8.2	1.26
i-butane	90	220	26	10.6	6.5	2.49
CO_2	35	100	34	13.8	7.0	1.84
CF_4	63	120	54	16.0	10.0	3.78

Figure 2: Caption for your image

TPCs usually contain a proportional counter, an electrical device that detects various types of ionizing radiation. Since the conditions of the detector are adjusted to the "proportional region", the voltage is high enough to produce electrons with sufficient acceleration and energy to ionize additional atoms in the medium and pass in a gas amplification procedure, also causing the avalanche effect. Using a special method that will be explained in chapter 4, those effects are filtered, eventually only the important signals remain intact.

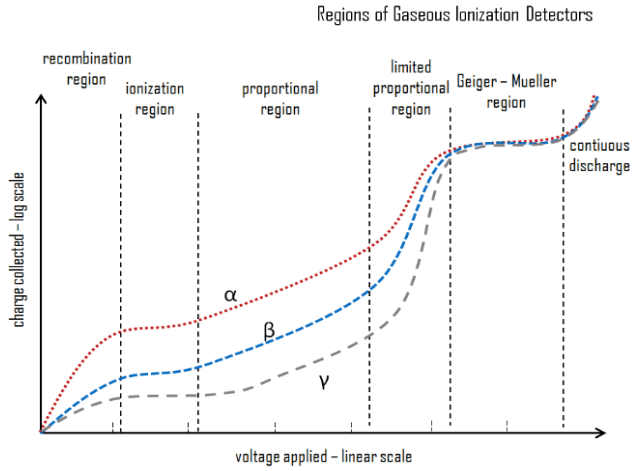

Figure 3: In this figure we notice the proportional region and the discrimination of the radiations based on their behavior as the voltage changes.

2.3 Drift velocities

In TPCs we aim for high drift speeds, since they allow charged particles to traverse the drift region quickly, reducing the time during which diffusion can blur the spatial information. This results in better spatial resolution when reconstructing the particle's trajectory. It also means that, we have a reduction in the diffusion effects and a higher precision in the localization of the particle's interaction points and trajectories. Apart from high spatial resolution, we obtain high temporal resolution too, since high drift speeds ensure that the ionization signal is collected before the particle undergoes decay or other interactions, especially for short-living particles. In that case, we prevent particles from interacting multiple times and we have more and clearer results in the end.

2.3.1 Drift of electrons

As electrons traverse through a gas, their light mass causes them to scatter uniformly losing their orientation after colliding with atoms. In the presence of an electric field E within the drift volume, electrons experience acceleration between collisions attaining a drift velocity u. This velocity is calculated by multiplying the acceleration by the average time since the last collision:

$$u_d = \frac{eE\tau}{m} = \mu E \tag{2.3.1}$$

where $\mu = \frac{e\tau}{m}$ is defined as the *mobility* factor, which is not a constant and τ is mean time between two collisions
While drifting, electrons can undergo many processes such as excitation, ionization and others. If we consider a number of collisions and the energy loss during them, we can describe the mean instantaneous velocity v as:

$$\frac{1}{\tau} = N\sigma v \tag{2.3.2}$$

where σ is the cross-section of the collisions and N is the density number of the gas molecules. Now, the total energy of an electron, including the thermal energy, is given:

$$\epsilon = \epsilon_E + \frac{3}{2}\epsilon = \frac{m}{2}v^2 \tag{2.3.3}$$

From equations 2.3.2 and 2.3.3, we get the final form of drift velocity:

$$v = \begin{cases} \frac{eE}{mN\sigma}\sqrt{\Delta/2}, \text{ for } \epsilon <= 3/2kT \text{ (cold gases: } CO_2) \\ \frac{eE}{mN\sigma}\sqrt{2/\Delta}, \text{ for } \epsilon >> 3/2kT \text{ (hot gases: } Ar \text{ and } CH_4) \end{cases} \tag{2.3.4}$$

where Δ is represents a fraction of the energy ϵ_E picked up between collisions. Technically, the first equation is used for reduced electric field drifts and the second one for high drift energies.
In TPCs we use either of the two equations based on the mixture of gases we use. The choice of gas and its properties, including σ and Δ, is critical for achieving high drift speeds in TPCs.

2.3.2 Drift of ions

For ions, we follow the same pattern. However, because of their heavier mass they have significant losses $\Delta \approx \frac{2m_iM}{(m_i+M)^2}$, where M is the gas molecule's mass, thus the diffusion will be much smaller and the mobility will be almost a constant for high electrical fields. The equation of the velocity becomes:

$$v_{rel}^2 = v_{ion}^2 + v_{gas}^2 = 3kT(m_i^{-1} + M^{-1}) \tag{2.3.5}$$

and with $\frac{1}{\tau} = N\sigma v_{rel}$ we have eventually:

$$v = \frac{eE}{N\sigma}(m_i^{-1} + M^{-1})^{1/2}(3kT)^{-1/2} \tag{2.3.6}$$

As we mentioned, in low E fields, v is relative to E/N and in higher E fields to $\sqrt{E/N}$

2.3.3 Effects of E/M fields on particles' drifts

The equation below, describes the drift velocity (v) of a charged particle in the presence of both electric (E) and magnetic (B) fields. Key parameters include the particle's mass (m), charge (e), and mean time between collisions (τ). The magnetic field effect is significant for electrons but negligible for ions.

$$v = \frac{e}{m}\tau\,|E|\left(\frac{1}{1+\omega^2\tau^2}\right)\left\{E^* + \omega\tau\,[E^* \times B^*] + \frac{\omega^2\tau^2(E^* \cdot B^*)}{B^*}\right\} \tag{2.3.7}$$

- E: Electric field vector.

- B: Magnetic field vector.
- E^* and B^*: Unit vectors in the direction of E and B respectively.
- ω: Cyclotron frequency, given by $\omega = \frac{e}{m}|B|$.

We will analyze only the case of the E field being almost parallel to the M field, since this is the case that best describes the conditions inside a TPC. The equations below describe the drift velocities of charged particles in a Time Projection Chamber (TPC) under the E/M conditions that we mentioned. From Langevin's relation 2.3.7, we find:

$$\frac{u_x}{u_z} = -\frac{\omega\tau B_y/B_z + \omega^2\tau^2 B_x/B_z}{1+\omega^2\tau^2} \tag{2.3.8}$$

$$\frac{u_y}{u_z} = \frac{\omega\tau B_x/B_z + \omega^2\tau^2 B_y/B_z}{1+\omega^2\tau^2} \tag{2.3.9}$$

These equations help more in understanding the displacement of particles in the x and y directions during the drift process.

2.4 Diffusion

Diffusion is the most important parameter to determine the gas mixture that we will use. Since diffusion refers to the spread of charged particles in all directions due to random collisions with gas molecules, the lower the diffusion is in gases the more it helps to minimize this spread during the drift, improving the spatial resolution of the TPC. We use the gaussian distribution to describe the density distribution N of the electrons drifting in the z-direction due to an E field:

$$N = (4\pi Dt)^{3/2} e^{-\frac{r^2}{4Dt}} \tag{2.4.1}$$

where D is the diffusion coefficient. In any direction from the center of the cloud, the mean squared deviation (σ: r.m.s. normal distance) of the electrons is:

$$\sigma_{||}^2 = \sqrt{2Dt} \tag{2.4.2}$$

and when the diffusion is transverse to the magnetic field:

$$\sigma_{\perp}^2 = \frac{\sigma_{||}^2}{1+\omega^2\tau^2} \tag{2.4.3}$$

where t is total time, $\omega = \frac{eB}{m_e}$ is the cyclotron frequency and τ is the mean collision time. At the figure below, figure 4 we can see pretty much how diffusion clouds look like in a gas chamber:

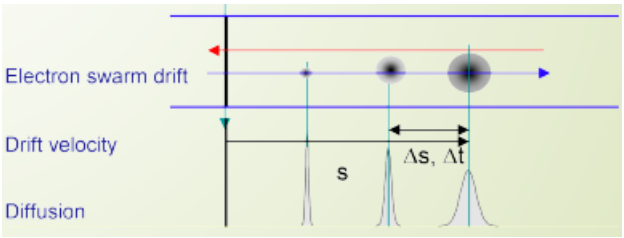

Figure 4: Diffusion of electrons and corresponding Gaussian plots

2.5 Summary of the theory

As far as the theoretical part is concerned, the factors that we need to take into consideration for the optimal operation of a TPC, are concentrated in the bullets bellow:

- Low Ionization energy: Gases with low ionization energies are preferred as they facilitate the ionization of particles passing through the gas, allowing efficient detection
- High Drift Velocity: Gases that allow high drift velocities for ionized particles are desirable. High drift velocities enable faster particle detection and better spatial resolution.
- Low Diffusion: Gases with low diffusion coefficients help minimize the spread of ionization electrons during the drift, improving the spatial resolution of the TPC.
- Magnetic Field Compatibility: If a magnetic field is present in the TPC setup, the gas should be chosen considering its compatibility with magnetic fields and any potential effects on particle trajectories.

Commonly used gases for TPCs include argon-based mixtures (e.g., Ar/CO_2 or Ar/CH_4) and xenon-based mixtures. These gases have favorable properties for particle detection and have been employed in various experimental setups.

3 Structure of a TPC

In this section, we will provide an overview of the fundamental structure of a Time Projection Chamber (TPC), along with examples of contemporary TPCs designed specifically for particle physics research.
The main parts of a TPC structure are below and also shown in figure 14:

- Large Gas Volume: For the interaction region which the particles will traverse.
- Field shaping electrodes: Shape the Electrical field inside the gas.
- Multi-Wire End-Cap Chamber Plane: A proportional counter that is located at one end of the gas volume and it consists of alternating anode and field wires. It plays a crucial role in collecting and amplifying the signals generated by ionization events.
- Cathode mesh: Separates the main gas volume from the end-cap chamber, allowing independent adjustment of the drift and multiplication fields. Controls the movement of charged particles.
- Printed Circuit board with Pad Rows: It is located on the outer part of the MWPC and its pad rows are parallel to the anodes. Their role is to collect the induced currents that are produced through the positive produced by the ionization trails.
- Solenoidal magnets: They produce the magnetic field in the gas bending the particles.

Technically, the whole procedure is based on the electrons that are released by the ionization trails inside the main gas volume. Those electrons drift towards the end-cap, they cross the mesh electrode and they are finally collected and amplified on the anode wires. In this way, they produce a negative signal on the anodes and a positive charge induction on the pad rows of the cathode. In total, the electric field within the TPC, generated by the potential difference between the anode and cathode, drives the charged particles towards the end caps and the combination with the magnetic field results in a helical motion for charged particles, aiding in their precise tracking and momentum measurement. So, at the end-caps is exactly where we obtain the (r,ϕ) reconstruction of the trajectory. One can observe the corresponding figures 6a and 6b below to understand better the procedure.
The major information that we get from a TPC, is the one that comes from MWPC plane, also known as azimuthial, provided by the pad rows which return not only the induced signal distribution-so called "pad response", but also the time that the produced electrons arrive at the pads, giving a 3-dimensional image of the particle's position. We will provide more details concerning this topic on chapter 4. Using those information one can determine the particle's type, localization and momentum, and as we mentioned, using

the proper gas filling we can reduce the diffusion and eventually acquire higher accuracy. Usually, we apply magnetic fields by adapting the detector in a solenoidal magnet.

The figures below show a basic TPC structure:

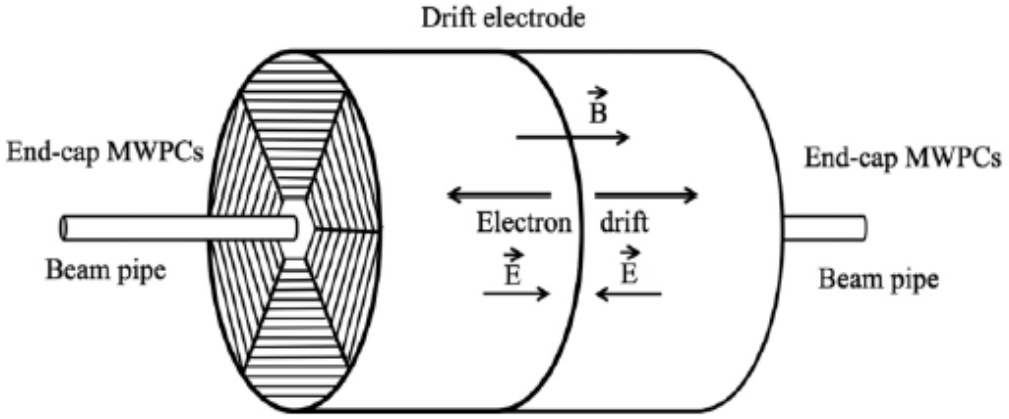

Figure 5: TPC Structure

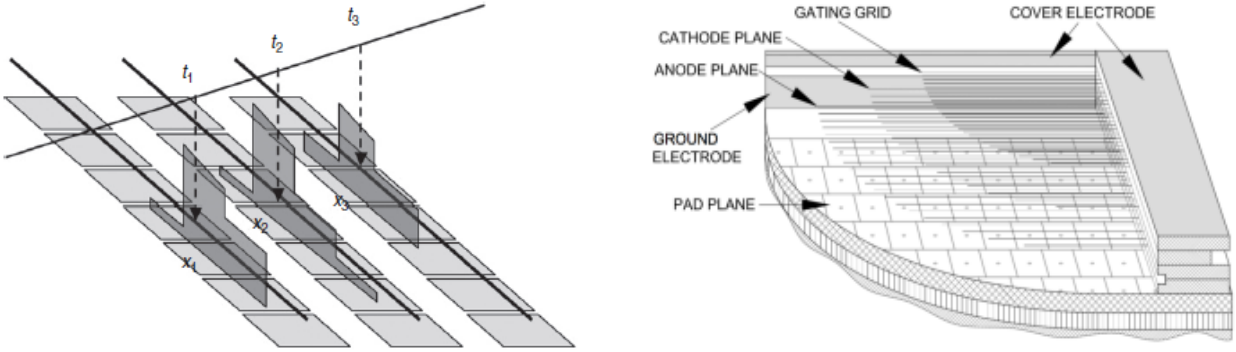

(a) Projection of the charge induction on the pad rows

(b) Trails produced through the ionization

Figure 6

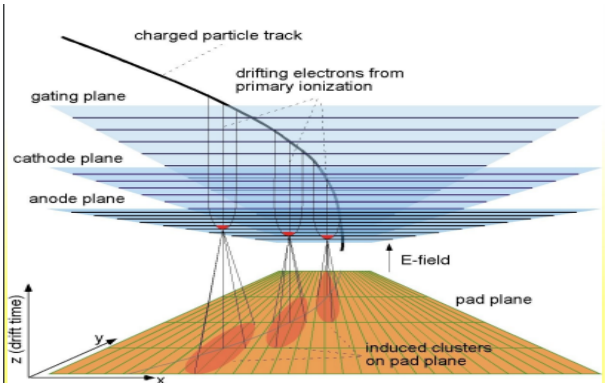

Figure 7: In this picture one can understand exactly how the signals are induced and reach the pads.

4 Readouts operation and results

It is important now to go through the full readout procedure and explain step-by-step the path to fully reconstruct the particles' trajectories.
As we already mentioned, the end-plates consist of a great number of finely segmented readout chambers - 557 568 pads = channels. When a particle transverses the medium and ionizes the gas around its trajectory, electrons are released. Those electrons are guided with the help of the E-field to the end-cap, where they leave their traces as signals on the pads. The signal is amplified and the arrival time is recorded for each pad. The initial particle's trajectory is curved because of the magnetic field inside the gas volume, thus we can get information and measurements about the particle's initial momentum. The density of the electron cloud allow us to identify the particle's type. In conclusion, the positions x-y from the projection of the electrons on the pads, and t their recorded arrival times, give a 3-dimensional image of the particle's trajectory in space. This corresponds approximately to a 500-Megapixel 3D camera that runs almost 200 frames per second.
The signal is amplified using the electron avalanche phenomenon. In the gas chamber the electrons are drifting across to an approximately straight field. The amplification happens close to the high gradient area (of the field) close to the wires. This happens, as the initial electron has enough energy to produce additional electron/ion pairs. The avalanche process creates a strong positive signal on the wire where the amplification occurs, which means that it can reduce or even cancel out any unwanted effects of capacitance couplings that may raise because of the closely spaced wires. In this way, the avalanche effect helps in improving the accuracy of the detected signals and the tracking resolution of the particle's trajectory. For a cylindrical TPC the equation for the radial perturbation of the electric field is given:

$$E(r) = \frac{\rho_0}{2\epsilon_0}\left(r - \frac{r_2^2 - r_1^2}{2rln(r_2/r_1)}\right) \tag{4.0.1}$$

In order to manage the ion feedback that might be produced from the avalanche effect, we have the Multi-Wire Proportional Chamber (MWPC) cathode and the drift volume.The gating grid can operate in two modes: always open or closed to ion flow, or always closed and open to ionization electrons. When the gate is open the grid wires have a voltage V_G and to close it we apply a symmetric ΔV_G field to the alternate wires. The gating technique proves to be effective in filtering the charges and optimizing the TPC performance. The image below shows exactly how the signal "filtering" occurs:

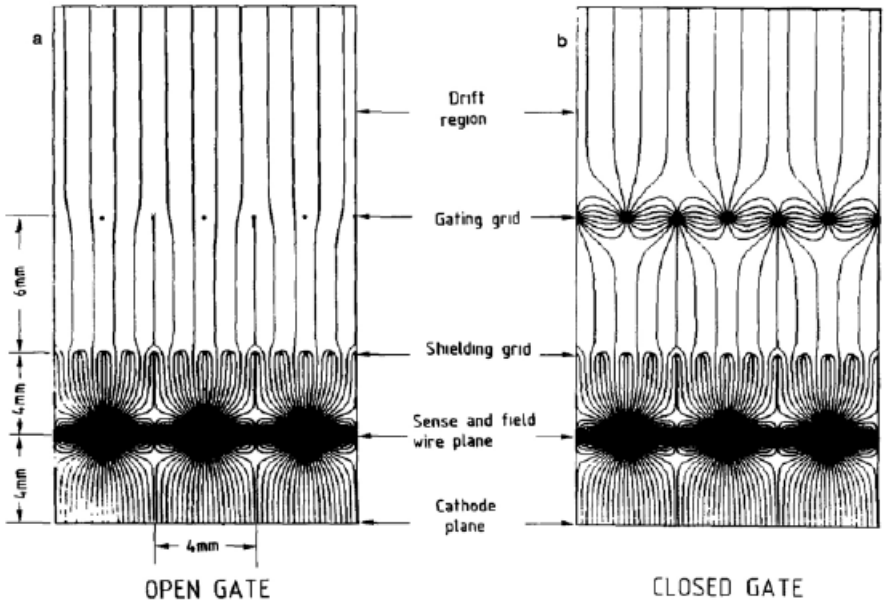

Figure 8: When the gate is closed it can block the ions that are generated from the interactions in the gas volume, from reaching the readouts (Amendolia et al., 1985a).

5 Signal Induction

After the "filtering" of the ions through the gating technique, the process involves multiplying charges on anodes, leading to induced charge profiles on facing pad rows. More specifically, if we have a look at the images in figure 6, we can observe the traces of particles left as induced signals on the pad rows. The charge induction profile on the cathode plane has a 2 dimensional-Gaussian-like shape, because of the avalanche effect, that evolves with time. In the x-direction parallel to the anode wire, the distribution is approximately given by the equation:

$$P(x) = e^{\frac{x^2}{2\sigma^2}}, \sigma = \frac{2G}{2.34} \tag{5.0.1}$$

where G is the gap size. The image below shows exactly this signal induction on the pad rows:

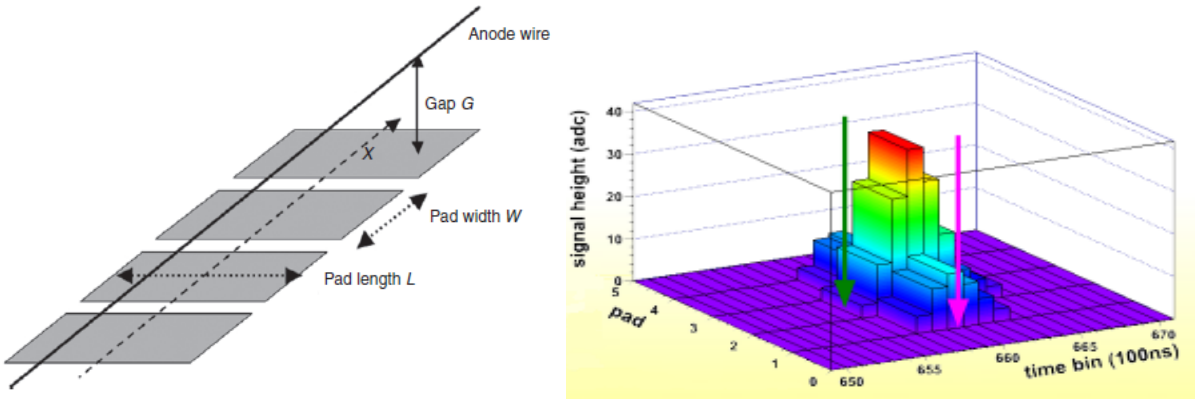

(a) Schematics of the pad rows geometry

(b) Signal evolution on a pad through time

Figure 9

This Gaussian-formed distribution, describes the spatial extent of the induced charge profile on the pad rows. In other words, it is the spatial distribution of induced charge around the position of ionization avalanches so from there we can determine the x-y position of the particle in 2D space. The third dimension is acquired from the drift measurements.

6 Laser calibration system

In large Time Projection Chambers, it is crucial to preserve a precise performance. This requires constant monitoring and thorough calibration. Using external sources, it is easy to monitor the proportional gain and the distortions/losses on the electron's drift lines.
A pulsed Laser is a quite powerful tool to perform tracking calibration. Nd:YAG lasers, N_2 laser of two stages, or pulsed N-lasers in general are quite capable of simulating straight tracks for tracking calibrations and offering controlled ionization and unaffected magnetic fields. This technique includes multiple lasers in fixed positions, spread all around the ionization volume. Fixed mirrors, splitters and remotely controlled rotating mirrors, are also included in the procedure.

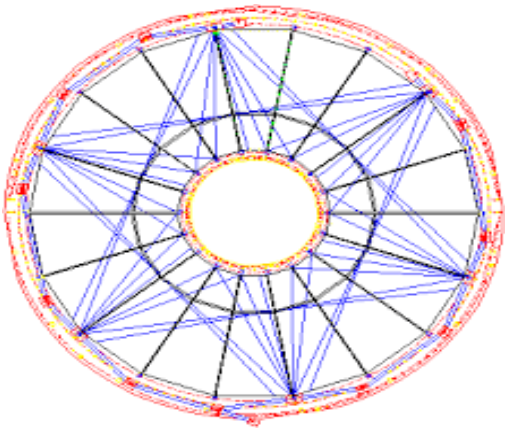

(a) Laser calibration system of TPC in ALICE

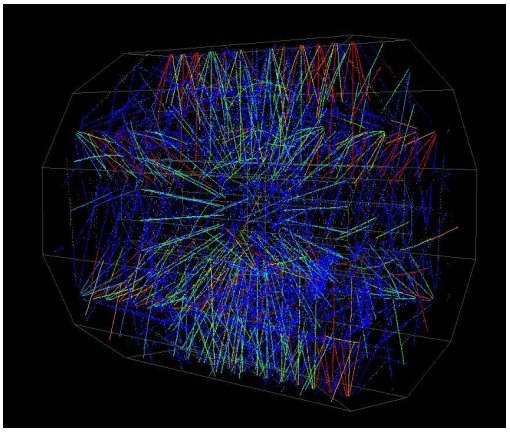

(b) The "Eye" picture generated from STAR TPC, in RHIC accelerator in USA. The calibration was performed with an ultraviolet laser beam.

Figure 10: Examples of laser calibrations in TPC devices.

The straight track reconstruction allows the corrections for mechanical tolerances, drift path distortions and temperature and gas variations and at the same time it provides a constant monitoring for the drift velocities.

7 Experiments using TPCs

Time projection chambers have been successfully employed in many particle and nuclear physics experiments around the world, providing accurate identification and imaging of the particles' types and trajectories. TPC examples particularly suitable for electron–positron storage rings such as the now-retired LEP at CERN and TRISTAN at KEK. Also, in low-rate fixed-target experiments such as, TRIUMF in Vancouver, very high multiplicity heavy ions at NA49 at CERN and STAR at RHIC and finally the gigantic ALICE TPC at CERN. However, other smaller TPC devices have been used in either particle or nuclear physics in many other forms (e.g. spherical TPCs, or TPCs that make use of liquid noble gases). In this section we will provide some more information about some characteristic cases of TPCs.

7.1 TPC-PEP4, SLAC

The TPC-PEP4 (Positron-Electron-Project) at SLAC, was the very first TPC prototype ever built. It was a project leaded by D. Nygren. The prototype was tested in the beam at LBL's Bevatron. To obtain higher resolution they moved to higher pressures up to 10 atmospheres. Some of its characteristics are presented below:

- Operation: 29 GeV e^+e^- collisions.
- Pressure: 8.5 Bar -it was an engineering challenge at that time.
- (r, ϕ) from induced signal on pads. 15 rows of 0.75 cm x 0.75 cm pads
- Anode wire readout
- The superconducting magnet vacuum vessel, was also the pressure vessel (quite ingenious)

Below you can see the corresponding design and an example of the results of the TPC:

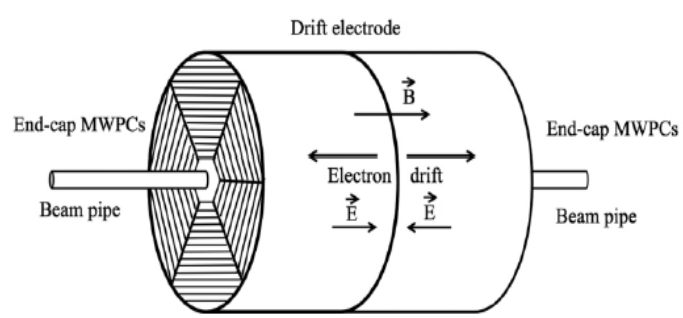

(a) TPC PEP-4, schematics -we used already this image as it is the simplest schematic to describe a TPC.

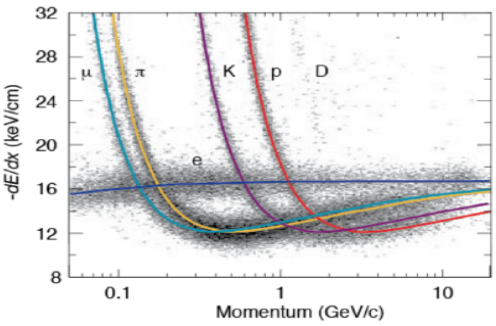

(b) Simulation of the particles' trajectories inside the chamber

Figure 11

In the figure 11 we can see the first identification results that ever come out using a TPC device. The results seem quite clear and trustworthy.

7.2 ALEPH TPC, LEP (CERN)

ALEPH TPC, is built at the Large Electron-Positron collider at CERN. It operated from 1989 to 1995 close to the energy range of the Z boson ($\approx 91 GeV$) and then from 1995 to 2000 above the threshold of W pair production (up to 200 GeV). Features:

- Dimensions: 4.4m length x 3.6m width.
- Magnetic field: 1.5 T produced by a superconducting coil on the outside of the tube.
- HCAL: Hadron Calorimeter with 4608 projective towers.
- ECAL: Electron Calorimeter with 73,728 projective towers, this means that it was meant to have the highest possible resolution for electron identification.
- It provides up to 330 ionization measurements per track.
- It includes an inner track chamber (ITC-drift chamber) and a silicon vertex detector.

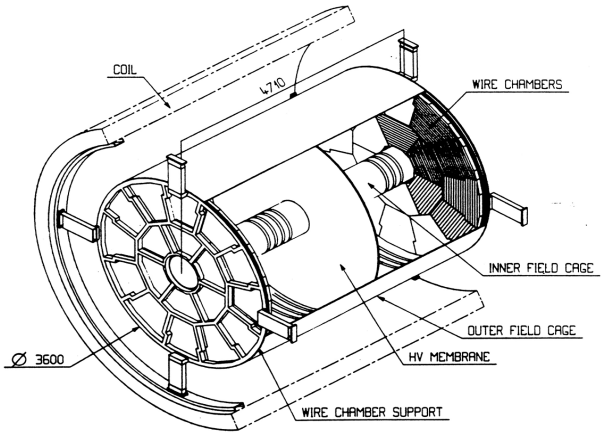

(a) TPC ALEPH, schematics

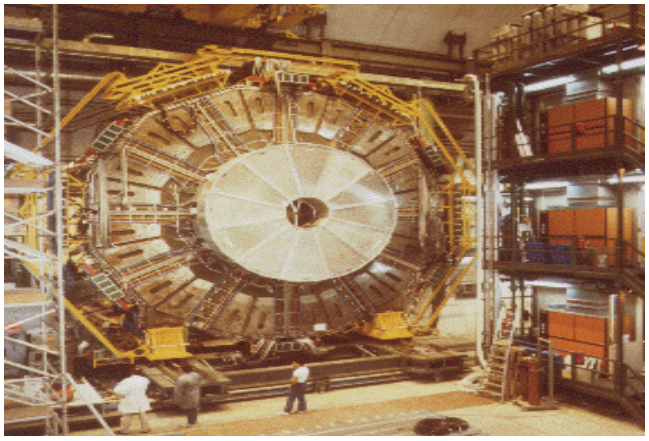

(b) One of the two End-Caps of ALEPH, CERN

Figure 12

Using the ALEPH TPC, CERN scientists were able to receive information about the decay products and reconstruct the energies and momenta of Z and later W bosons, and eventually calculate their masses. ALEPH, also contributed in the measurement of the coupling constant α_s of the strong interactions (QCD), more specifically it measured α_s for low energies close to τ lepton mass (1.77 GeV) and for high energies close to Z boson mass (91.19 GeV).

7.3 TPC Alice, CERN

The TPC in ALICE experiment, at CERN, is one of the most significant challenges in the history of TPC detectors. Its dimensions are 5.6m diameter (Outer containment vessel) and 5.2m length. It is the main tracking and particle identification detector inside the barrel of the ALICE experiment. Some important features of the device, are found below:

- Gas Volume: 90 m^3.
- Gas type: $Ar - CO_2$ in atmospheric pressure, $Ne - CO_2$ and $Ne - CO_2 - N_2$ -Cold gas- Low diffusion.
- MWPCs with 2x18 Inner readout chambers and 2x18 outer readout chambers with a total number of 557 568 readout pads.
- Drift field: $400V/cm$ - central cathode at 100 kV
- Resolution on each of the coordinates x,y and z: $200\mu m$
- Magnetic field: 0.5T

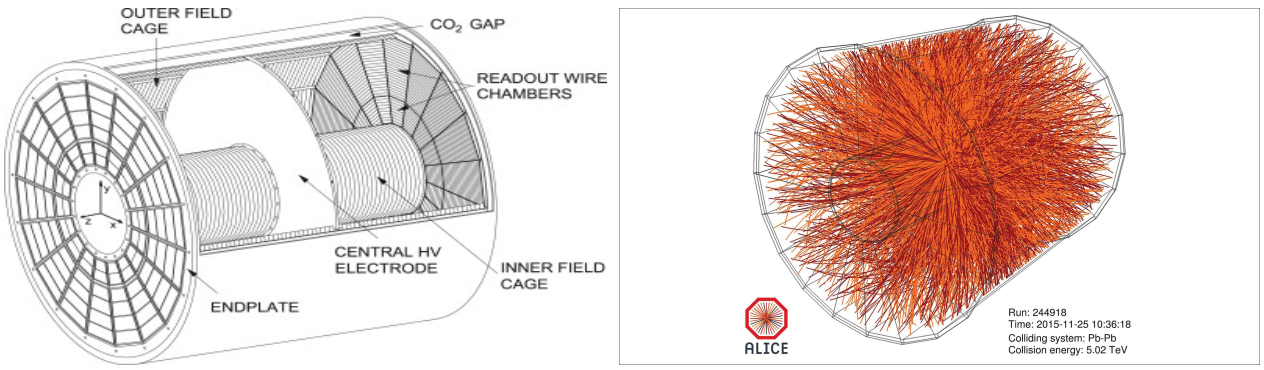

(a) TPC ALICE, schematics

(b) Simulation of the particles' trajectories inside the chamber

Figure 13

The TPC in ALICE experiment needs to operate at temperatures very close to 0 K, which means that it has a very demanding and complex cooling system. It consists of about 60 adjustable cooling circuits and at least 500 temperature sensors all over the TPC that monitor the system. They are calibrated at 100 mK (very high accuracy). Some of their final results are found below:

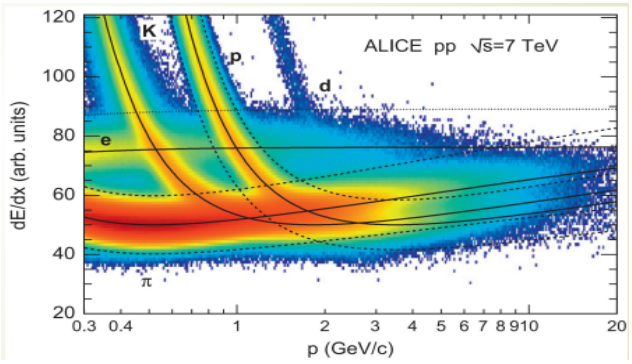

Figure 14: Final results of the particle identification in ALICE experiment

In total, the identification of the charged particles is easily achieved by measuring simultaneously the momentum and their dE/dx.

7.3.1 ZEPLIN-III

One of the newest TPC based experiments, nowadays, is the ZEPLIN-III (ZonEd Proportional scintillation in LIquid Noble gases) at Boulby Underground Laboratory in Loftus, Yorkshire, and its dedicated to dark matter exploration. Its purpose is located specifically, in the detection of galactic WIMPs (Weakly interacting massive particles), using a 12 kg liquid Xenon target. It operated from 2006 to 2011 and the whole ZEPLIN-III project was led by the Imperial college London, and included collaborations with other famous laboratories around the world (Rutherford Appleton Laboratory, University of Edinburgh, LIP-Coimbra in Portugal and ITEP-Moscow). Before ZEPLIN-III, ZEPLIN-I and II were developed starting from the 1990's using smaller amounts of liquid detecting materials. Liquid noble gas detectors have a quite different but at the same time similar structure as a classic TPC system. Xenon and Argon condensed noble gases (liquid forms) are excellent radiation detection media and that is exactly what is needed for dark matter search.
Features of ZEPLIN-III:

- As most of the liquid noble gas based TPCs, ZEPLIN-III has the ability of getting information about the **ionization** of the particle and the **scintillation** (when a particle enters it interacts with the liquid and emits photons in visible or ultraviolet scale).
- 31 photomultipliers: They receive the signals from the scintillation in the liquid as well as the delayed electroluminescence (electrical/optical phenomenon where the material emits light when a strong electrical field or a current transverses it).
- Two chambers in a cryostat vessel: The upper one contains 12 kg of liquid Xenon and the array with the 31 photomultipliers we mentioned above. The lower one contains liquid nitrogen for the cooling system.
- It is built mainly of Copper but it is shielded with Gd-loaded polypropylene to capture neutrons and minimize the potential background sources, and with another layer of 20cm of lead.
- The gamma rays of the neutron capture are registered in 52 plastic scintillator modules located around the moderator (Polypropylene layer).

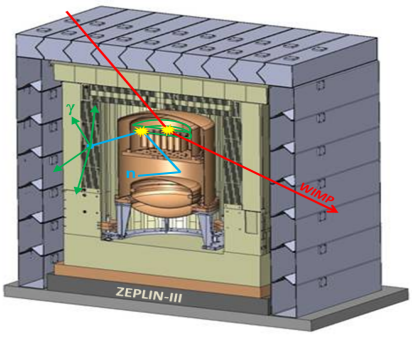

(a) ZEPLIN-III, schematics

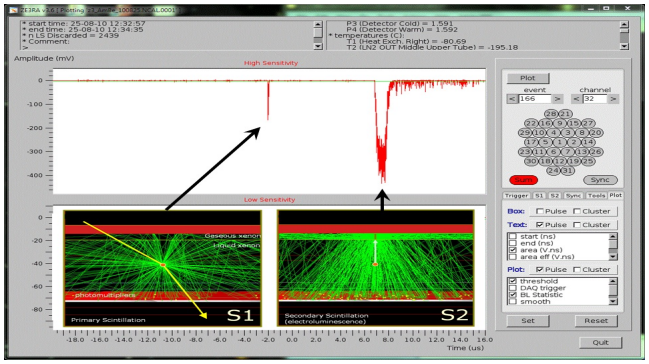

(b) Signals and simulations of the events in ZEPLIN-III. On the upper image the first pulse (S1) comes from the scintillation in the liquid, and the second delayed pulse (S2) is generated by the ionization drifted at the interaction point in the gas above the liquid. The images below are Monte-Carlo generated simulations for the optical signals.

Figure 15

As technology evolves, ZEPLIN-III has confirmed that TPC devices have set the foundation for further research and development in detection systems. From high energy physics to astrophysics, the concept on detection systems doesn't really change. ZEPLIN-III's results have contributed valuable insights into WIMP-nucleon interactions, and of course it will continue to inspire engineers in the future.

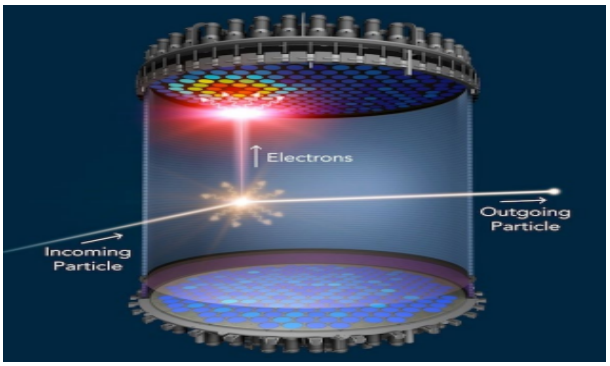

(a) LUX-ZEPLIN (LZ) experiment, schematics

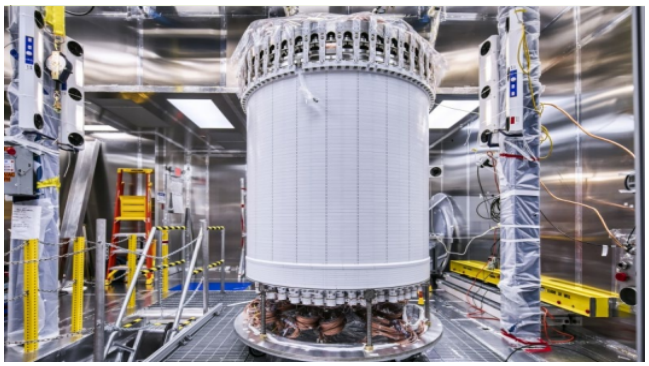

(b) LUX-ZEPLIN (LZ) experiment, next generation ZEPLIN experiment using 7000kc of liquid Xenon, has started its development.

Figure 16

To be continued ...

8 Summary

Time Projection Chambers are huge volumes in any geometry filled with gas or liquid detection medium, and using the effect of ionization and drift of electrons in a uniform E/M field, they can provide the 2D projection of the particles trajectories. Taking advantage of the time recorder for the drift electrons they also provide the third coordinate. Thus, we end up with a 3D reconstruction of the particle trajectory. The evolution of TPC technology has been remarkable, enhancing particle identification and resolution capabilities.
In conclusion, TPCs provide a complete 3-dimensional reconstruction of particle trajectories, offering a comprehensive view of their paths, offering precise insights. Based on the geometry or the type of a TPC, they

are easily adaptable to various experimental setups. However, challenges for TPCs nowadays, concern their size, design and maintenance complexity and even the the huge amount of substantial data that need to be properly handled. There may also be limitations in the rate at which they can process information due to issues like attachments or diffusions, affecting drift time.
In the face of these challenges, scientists have faith and continue to research and push their boundaries in experimentation. The enigma of the universe continues to inspire ingenious research, prompting the invention of new technologies and methodologies. This evolving landscape of unanswered questions serves not as an obstacle, but as a motivation for further exploration, inviting scientists to push the boundaries of their knowledge to unknown territories more and more.

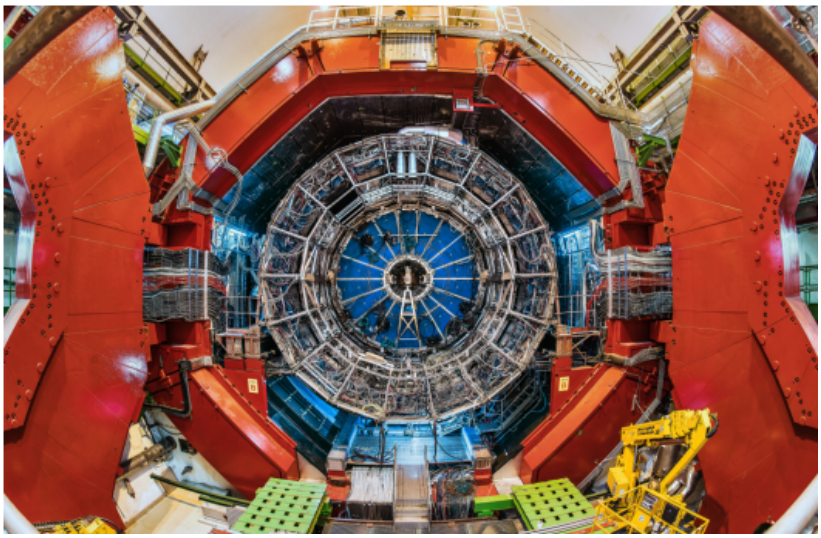

Figure 17: Image from TPC, ALICE experiment at CERN

9 Questions that raised during the research

- Would it be possible to automate the identification procedure by training a neural network to recognise the momentum and the approximate trajectories and distinguish instantly the particles? This would make the analysis faster and the search for new physics easier.
- How far can TPC technology go? How can we use those technologies for human-orientated purposes?
- Is TPC technology that promising in discovering dark energy? Is it also promising to use this idea for Beyond Standard Model physics?

References

[1] Fabio Sauli (2014), *Gaseous Radiation Detectors: Fundamentals and Applications.*(Cambridge Monographs on Particle Physics, Nuclear Physics and Cosmology, pp. 292-326) https://www.cambridge.org/core/books/abs/gaseous-radiation-detectors/time-projection-chambers/1D64201C6DCBF43D3501852EF7530D05

[2] H. J. HILKE (2010), *Time Projection Chambers.* (CERN) https://cds.cern.ch/record/1302071/files/CERN-PH-EP-2010-047.pdf

[3] Abbrescia, M., et al. (2013), *Gaseous Detectors.* https://indico.cern.ch/event/1224299/contributions/5259875/attachments/2685206/4658622/Abbrescia@Wuppertal_v2.pdf

[4] Sirvent-Blasco, J. L. (2019), *Mean energy loss rate in liquid hydrogen, gaseous helium, carbon, aluminium, iron, tin and lead.* https://www.researchgate.net/figure/Mean-energy-loss-rate-in-liquid-hydrogen-gaseous-helium-carbon-aluminium-iron-tin_fig27_331284711

[5] Jens Wiechula (2013), *Everything you wanted to know about TPC but where afraid to ask.* https://alice-analysis.web.cern.ch/sites/default/files/documents/Analysis/JensJD.pdf

[6] Wikipedia (last edited on 2022), *ZEPLIN-III.* https://en.wikipedia.org/wiki/ZEPLIN-III

[7] LZ Dark Matter Experiment (2020), *LZ Dark Matter Experiment – LZUK.* http://lz.ac.uk/lz-experiment/

[8] Ezra D. Lesser (2021), *Time Projection Chambers (TPCs) and applications.* https://indico.physics.lbl.gov/event/1474/contributions/5689/attachments/2718/3574/Time%20Projection%20Chambers%20%28TPCs%29%20and%20applications.pdf

[9] Nick Connor. *Proportional Counter – Proportional Detector – Definition.* December 14, 2019. https://www.radiation-dosimetry.org/what-is-proportional-counter-proportional-detector-definition/

[10] Institute of Physics, Justus-Liebig-univeritat Geissen *A former project: the "Eye" Picture.* https://www.uni-giessen.de/de/fbz/fb07/fachgebiete/physik/institute/iipi/arbeitsgruppen/ag-kuhn/forschung-kuehn/eye-picture

[11] Alexander Deisting (2019), *The ALICE Time Projection Chamber and its upgrade* https://www.hep.ph.ic.ac.uk/seminars/slides/2019/190130_Deisting_ALICE_Hardware.pdf

[12] ALEPH, LEP (CERN) *Official website.* https://aleph.web.cern.ch/aleph/aleph/newpub/physics.html